Effects of Hydrogen and Weld Defect on Tensile Properties of SUH660 and SUS316L Welded Joints

Masanobu Kubota and Ryosuke Komoda
International Institute for Carbon-Neutral Energy Research (WPI-I2CNER), Kyushu University, Fukuoka, Japan
Email: kubota.masanobu.304@m.kysuhu-u.ac.jp, komoda6744@kyudai.jp

Xuesong Cui
Graduate School of Kyushu University, Fukuoka, Japan
Email: 2TE16719M@s.kyushu-u.ac.jp

Hiroshi Wakabayashi and Yasuhisa Tanaka
Nagano Keiki, Ueda, Japan
Email: h_wakabayashi-m@naganokeiki.co.jp, y_tanaka-m@naganokeiki.co.jp

***Abstract*—The effect of hydrogen on the tensile properties of the SUH660 and SUS316L different materials welded joints was characterized in conjunction with the joint shape and weld defects. The butt welded joint specimen without weld defect fractured at the SUS316L base material, and did not cause hydrogen embrittlement (HE). However, the failure position of the spigot-lap welded joint specimen moved from the SUS316L base material to the weld part when hydrogen charging was applied. This resulted in a significant reduction of the elongation. It was presumed that the HE was induced by the stress concentration due to the weld shape. The weld defect induced HE in both joints. The weld defect was produced by incomplete penetration. It also caused incomplete mixing of the weld metal. Consequently, filler nickel segregated around the weld defect, then HE occurred.**

***Index Terms*—hydrogen, weld joint, different materials weld, tensile properties, weld defect**

I. Introduction

Since hydrogen for fuel cell vehicles (FCV) was introduced into the market in Japan in 2014, numbers of FCV and hydrogen refueling stations (HRS) are growing. Application of welding to high-pressure hydrogen service systems instead of mechanical joints is a promising way to reduce the cost of the systems, and contribute to accelerate spread of FCV and HRS. Therefore, characterization of the hydrogen embrittlement of welded joint is extensively studied. For the hydrogen compatibility of the welds of austenitic stainless steels, the effects of α'-martensite [1], nickel content [2, 3], sensitization [2], γ'-precipitates [4], weld defect [5], dendrite microstructure [6], δ-ferrite [6], etc. were discussed. In this study, a welded joint consists of different materials is studied. The objective is to characterize the effects of hydrogen on the tensile strength properties of the welded joints of different materials.

II. Experimental Procedure

A. Material

The materials of the weld joints were JIS SUH660 precipitation-hardened stainless steel and JIS SUS316L austenitic stainless steel. It is known that the SSRT properties of SUH660 do not deteriorate in high-pressure hydrogen gas [7]. However, its hydrogen-charged material suffers from hydrogen embrittlement (HE) [8]. SUS316L has a good hydrogen compatibility in the SSRT [9].

B. Hydrogen Charging

The effect of hydrogen was investigated by hydrogen-charged specimens. The specimens were exposed to 107 MPa hydrogen gas at 543 K for 69.5 h. Based on the diffusivities of hydrogen in these metals and the hydrogen charging conditions, it can be considered that hydrogen was uniformly distributed throughout the specimen diameter. The resulting hydrogen contents measured by the thermal desorption analysis were 92 mass ppm for the SUH660, 96 mass ppm for the weld part, and 98 mass ppm for the SUS316L.

C. Tensile Test

When considering high-pressure hydrogen gas containment systems, hoop stress due to internal pressure

Manuscript received June 8, 2018; revised July 5, 2019.

doi: 10.18178/ijmerr.8.5.713-718

could dominate the fracture of the structure. However, tensile tests of the welded joints were carried out in this study in order to achieve a basic understanding of the effect of hydrogen on the strength properties of the welded joints. The tensile tests of the hydrogen charged and uncharged weld joints were carried out in air at room temperature with a strain rate of 5×10^{-5} 1/s. The elongation was measured by an extensometer with a 24-mm gauge length.

D. Weld Joint Specimen

The shapes of the specimens are shown in Fig. 1. Two types of welding methods, simple butt welding and spigot-lap welding, were used. There was an unwelded part in the spigot welded joint as shown in Fig. 1 (c) and it caused a stress concentration during tensile loading. For the explanation, the results of simple elastic FEM calculations of these welded joints receiving tensile loading are shown in Fig. 2. Thus the spigot joint was used to investigate the overlapping effect of stress concentration and hydrogen. The welding used a nickel filler. An electron beam welding was used. An artificial small weld defect was introduced into some specimens by applying an incomplete penetration condition in order to investigate the synergetic effect of the weld defect and hydrogen.

Fig. 3 shows the microstructure and hardness distribution at the weld part. The hardness of the SUH660 started to reduce approximately 1 mm from the weld part. When a re-aging heat treatment was applied to the weld joint, the reduced hardness recovered to the initial hardness before the welding. Therefore, the reason for the reduced hardness was dissolving of the precipitates by the heating during the welding. The hardness of the weld part was almost the same as that of the SUS316L base material.

III. Results of Tensile Tests and Discussion

Table I summarizes the results of the experiment. Fig. 4 shows the nominal stress and nominal strain curves. For the uncharged non-artificial defect specimens, the fracture occurred at the nominal part in both the butt and spigot welded joints. For the uncharged artificial defect specimens, the fracture of the butt joint occurred at the nominal part, but the fracture of the spigot joint occurred at the weld part. Therefore, the small artificial defect did not affect the fracture alone, but affected the fracture when the stress concentration of the unwelded notch overlapped.

For the hydrogen-charged non-artificial defect specimens, the fracture of the butt welded joint occurred at the nominal part, but the fracture of the spigot welded joint occurred at the weld part. In the former case, there was no HE as shown in Fig. 4 (a). On the other hand, in the latter case, reduction of the elongation was significant as shown in Fig. 4 (b). The weld joint shape affected the results that whether or not HE occurred.

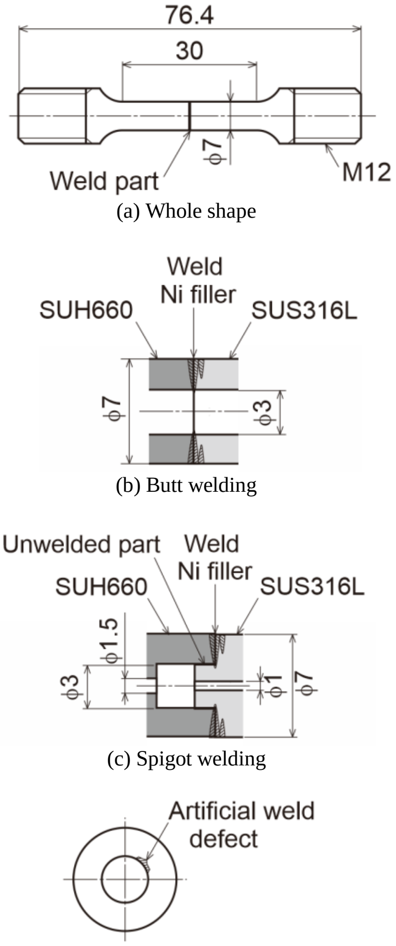

(a) Whole shape

(b) Butt welding

(c) Spigot welding

(d) Artificial defect

Figure 1. Tensile test specimen.

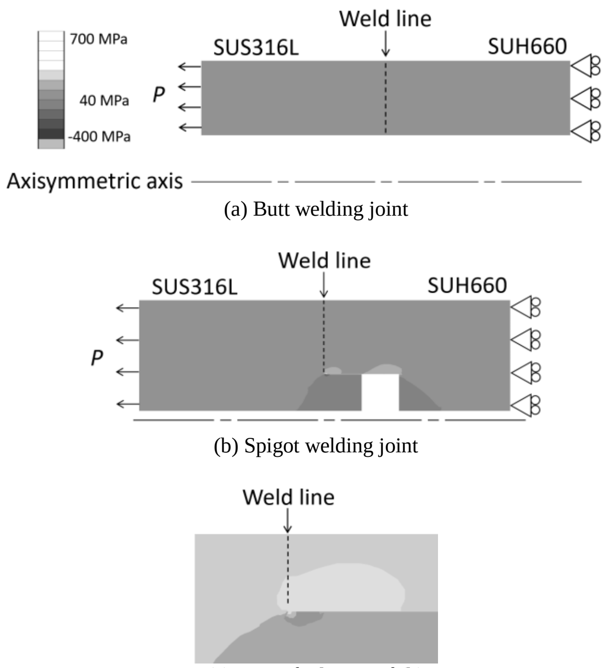

(a) Butt welding joint

(b) Spigot welding joint

(c) Magnified view of (b)

Figure 2. Axial stress distribution of the welding joints during tensile loading (Elastic finite element analysis, Axisymmetric, Young's modulus E = 200 MPa, Poisson's ratio ν = 0.3).

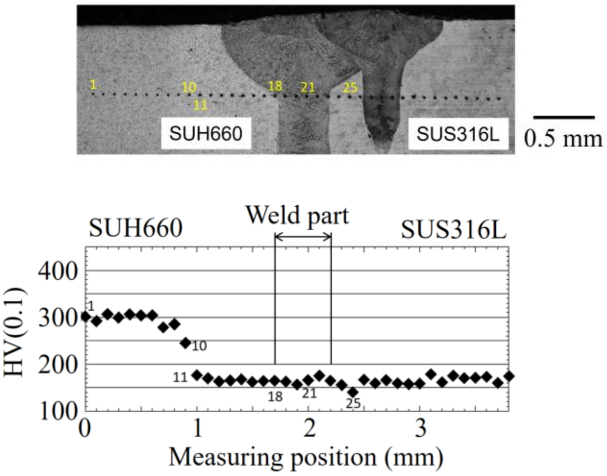

Figure 3. Microstructure and hardness of the weld part.

In Fig. 4, there was no quantitative meaning of the measured strain by the extensometer since the different materials having different yield strength were included within the gauge length. Therefore, local deformation was also measured by a digital image correlation (DIC) method in some tensile tests. For the results of Fig. 4 (d), the results of the DIC is shown in Fig 5. The same conclusion that HE occurred was obtained.

The crack originated from the unwelded notch root in the uncharged spigot welded joint and propagated along the boundary between the weld metal and SUS316L base material as shown in Fig. 6. The most of the fracture surface showed a dimple. Fig. 7 shows the same observation of the hydrogen-charged spigot weld joint specimen. The crack path was the same as that of the uncharged one. However, the fracture surface of the hydrogen-charged specimen consisted of intergranular cracking (IGC), quasi-cleavage (QC) and dimple.

It is known that a SUS316L smooth specimen shows a good resistance to HE. However, reductions of the fracture toughness and notch tensile strength of similar stainless steels (AISI 316L [10] and Type 316L [11]) were reported. In the case of the spigot welded joint specimen, the unwelded notch caused a similar stress conditions. As a result, the HE and consequent change in the fracture position occurred. Additionally, the HE of the similar alloy welds was reported with specific welding parameters [2]. The effect of welding parameters is future research subject in this study.

For the artificial weld defect specimens, the fracture position of the butt welded specimen changed from the nominal part to the weld part by the hydrogen charge. This resulted in a significant reduction of the elongation. Since the non-defect butt welded joint specimen did not cause HE, the defect induced the hydrogen effect. However, the primary reason was not stress concentration of the weld defect, but was nickel segregation as descried later. The fracture surface of the hydrogen-charged artificial-weld defect butt welded specimen is shown in Fig. 8. The IGC adjacent to the artificial defect was clearly found. Since the IGC of the SUS316L due to

TABLE I. RESULTS OF TENSILE TEST

Non-artificial weld defect	
Butt welding	
Uncharged	Broken at nominal part 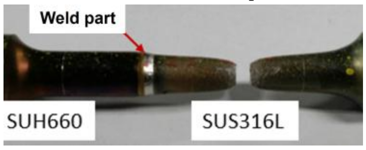 UTS = 488 MPa, Elongation 39 %
Hydrogen charged	Broken at nominal part 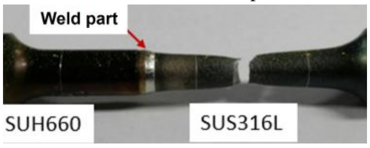 UTS = 532 MPa, Elongation 39 %
Spigot welding	
Uncharged	Broken at nominal part 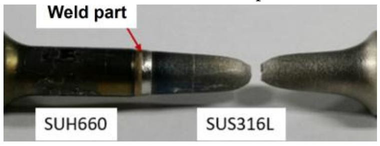 UTS = 500 MPa, Elongation 40 %,
Hydrogen charged	Broken at weld part  UTS = 496 MPa, Elongation 25 %
Artificial weld defect	
Butt welding	
Uncharged	Broken at nominal part 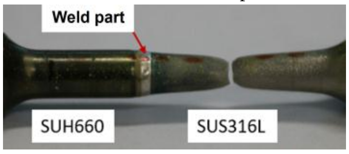 UTS = 478 MPa, Elongation 38 %
Hydrogen charged	Broken at weld part 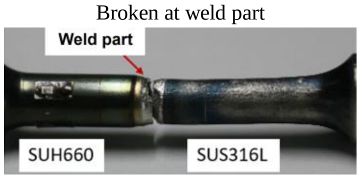 UTS = 475 MPa, Elongation 21 %
Spigot welding	
Uncharged	Broken at weld part 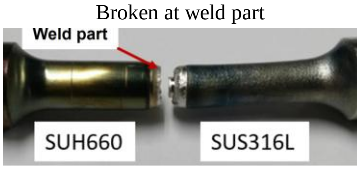 UTS = 458 MPa, Elongation 22 %
Hydrogen Charged	Broken at weld part 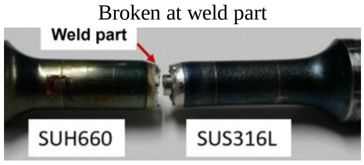 UTS = 462 MPa, Elongation 15 %

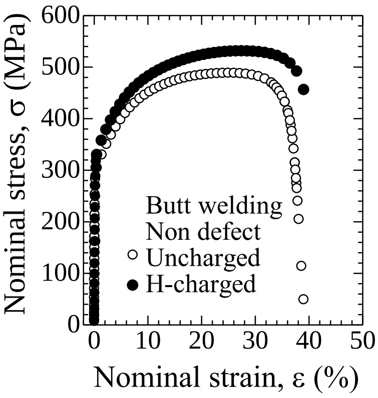

(a) Butt joint, Non defect

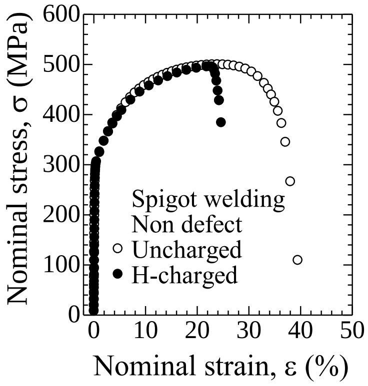

(b) Spigot joint, Non defect

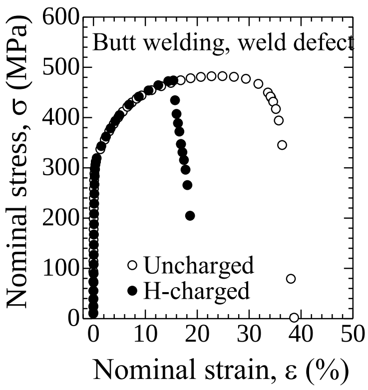

(c) Butt joint, Weld defect

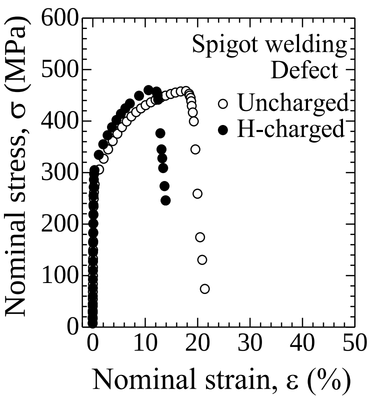

(d) Spigot joint, Weld defect

Figure 4. Stress-strain curves.

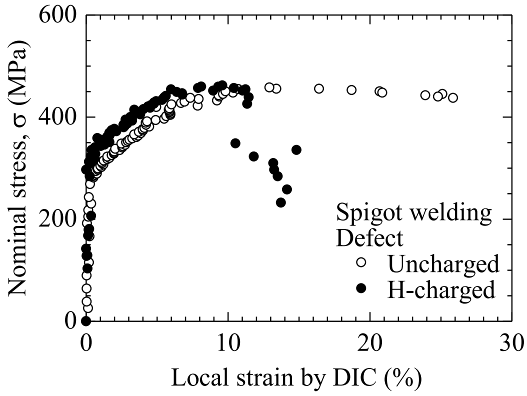

(a) Nominal stress – local strain curves

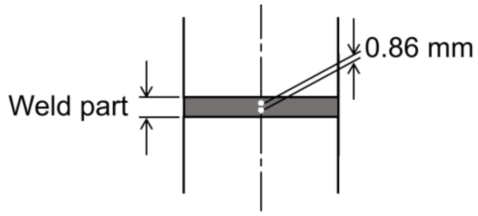

(b) Refference points for DIC

Figure 5. Stress-strain curves of the artificial defect spigot lap weld joint specimen obtained by DIC.

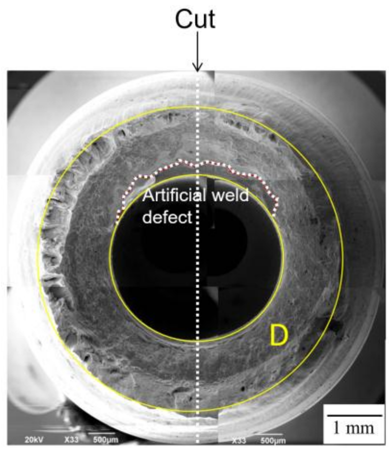

(a) Fracture surface and cutting position

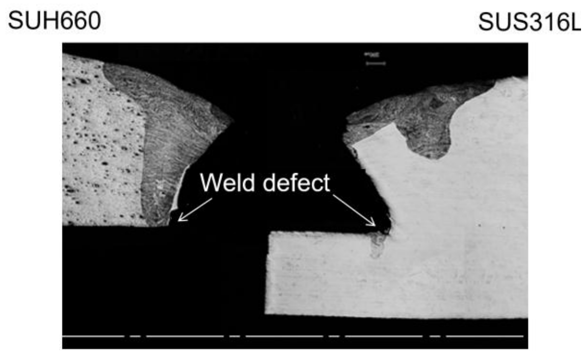

(b) Longitudinal section of the specimen

Figure 6. Observation of crack path of the uncharged spigot lap welding joint specimen.

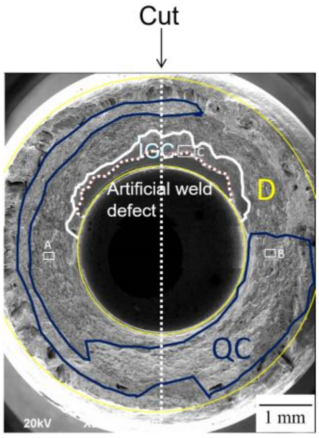

(a) Fracture surface and cutting position

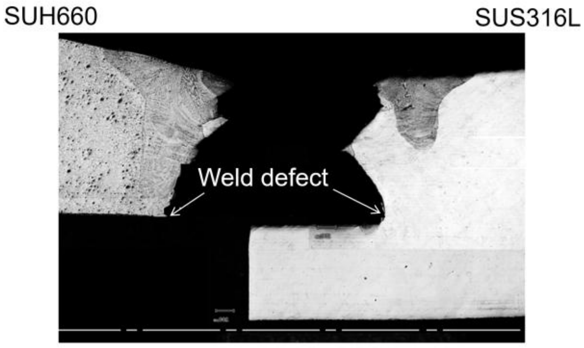

(b) Longitudinal section of the specimen

Figure 7. Observation of crack path of the hydrogen-charged spigot lap welding joint specimen.

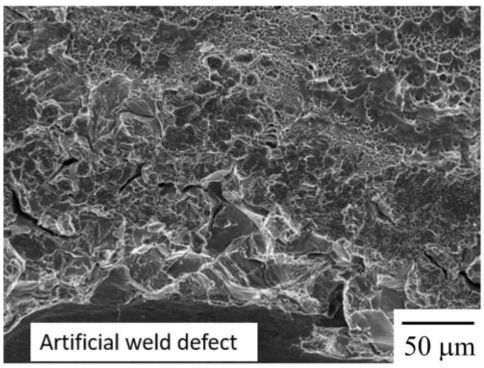

(a) Intergranular cracking

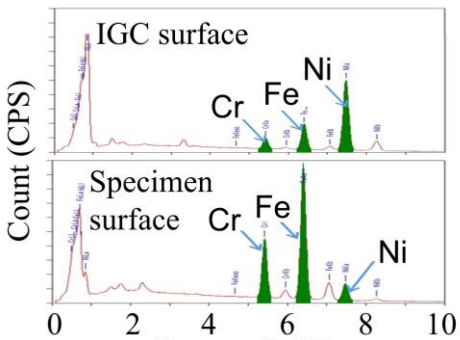

(b) EDS surface analysis

Figure 8. Intergranular cracking observed in the hydrogen-charged artificial weld defect butt welded specimen and the results of EDS surface analysis.

hydrogen seemed to be unusual, the reason for the IGC was investigated. Fig. 8 also shows the results of the surface composition analysis by Energy Dispersive X-ray spectroscopy (EDS). The intensity of the nickel was significantly higher on the IGC fracture surface compared to that on the specimen surface. On the other hand, there are many studies that nickel [12] and a nickel-based super alloy [13] cause the IGC by hydrogen. Therefore, in this study, the insufficient penetration to produce the small weld defect also caused insufficient mixing of the nickel filler. Consequently, the IGC occurred in the vicinity of the weld defect where the nickel segregated.

IV. Summary

The effect of hydrogen on the tensile properties of the SUH660 and SUS316L welded joints consisting of different materials was characterized. The butt welded joint without weld defect did not suffer from HE. On the other hand, the spigot-lap welded joint and the butt welded joint with a weld defect caused HE. The weld defect and stress concentration due to the weld joint shape had a significant impact on the resistance to HE of the weld joint.

References

[1] X. Li, B. Gong, C. Deng, and Y. Li, "Failure mechanism transition of hydrogen embrittlement in AISI 304 K-TIG weld metal under tensile loading," *Corrosion Science*, vol. 130, pp. 241-251, January 2018.

[2] L. A. Hughes, B. P. Somerday, D. K. Balch, and C. San Marchi, "Hydrogen compatibility of austenitic stainless steel tubing and orbital tube welds," *Hydrogen Energy*, vol. 39, pp. 20585-20590, December 2014.

[3] S. Matsuoka, T. Sato, N. Yamaguchi, S. Hamada, M. Nakamura, and H. Matsunaga, "SSRT properties of austenitic stainless steel weld metals in hydrogen gas at -45 ℃ and 106 MPa," *Trans JSME*, vol. 82, no. 839, pp. 1-19, July 2016.

[4] Y. Yan, Y. Yan, Y. He, J. Li, Y. Su, and L. Qiao, "Hydrogen-induced cracking mechanism of precipitation strengthened austenitic stainless steel weldment," *Hydrogen Energy*, vol. 40, pp. 2404-2414, February 2015.

[5] Y. Matsumoto, M. Kubota, and Y. Kondo, "Effects of small defect and hydrogen on fatigue strength of weld-jointed tube in austenitic stainless steel," *Trans JSME, Ser. A.* vol. 77, no. 781, pp. 1554-1558, September 2011,

[6] M. Nakamura, S. Okazaki, H. Matsunaga, and S. Matsuoka, "SSRT and fatigue life properties of austenitic stainless steel weld metal 317L in high-pressure hydrogen gas," *Trans JSME*, vol. 84 no. 857, pp. 1-20, 2018.

[7] Safety Standard for Hydrogen and Hydrogen Systems, Guidelines for Hydrogen System Design, Materials Selection, Operations, Storage, and Transportation, National Aeronautics and Space Administration, NSS 1740.16, 1997.

[8] N. Tajima, A. Orita, T. Matsuo, Y. Yamaguchi, J. Yamabe, and S. Matsuoka, "Effect of internal hydrogen on tensile properties of iron-based superalloy SUH 660," *Trans. JSME*, vol. 78, no. 792, pp. 1173-1188, 2012.

[9] T. Omura, H. Hirata, M. Miyahara, and T. Kudo, "Effect of chemical compositions on embrittlement properties of stainless steels in highly pressurized gaseous hydrogen environments," *Zairyo-to-Kankyo*, vol. 57, no.1, pp. 30-36, January 2008.

[10] A. Valiente, L. Caballero and J. Ruiz, *Nuclear Engineering and Design*, vol. 188, pp. 203-216, 1999.

[11] E. J. Song, S. W. Baek, S. H. Nahm, and U. B. Baek, "Notched-tensile properties under high-pressure gaseous hydrogen: Comparison of pipeline steel X70 and austenitic stainless type 304L, 316L steels," *Hydrogen Energy*, vol. 42, pp. 8075-8082, March 2017.

[12] M. L. Martin, B. P. Somerday, R. O. Ritchie, P. Sofronis and I. M. Robertson, “Hydrogen-induced intergranular failure in nickel revisited,” *Acta Materialia*, vol. 60, pp. 2739-2745, April 2012.
[13] M. C. Rezende, L.S. Araujo, S.B. Gabriel, D.S. dos Santos, L.H. de Almeida, “Hydrogen embrittlement in nickel-based superalloy 718: Relationship between γ'+ γ" precipitation and the fracture mode,” *Hydrogen Energy*, vol. 40, pp. 17075-17083.

Masanobu Kubota was born in Nagano, Japan, in 1970. He received BS and MS in Engineering from the University of Electro-Communications in Tokyo, Japan in 1992 and 1994, respectively. He received PhD in Engineering from Kyushu University in Fukuoka, Japan in 2001. His specialties are fatigue and fracture, fretting fatigue and hydrogen embrittlement. He worked as an assistant professor at Kyushu University from 1996 to 2010. Then he began an independent carrier as a professor since 2010 in Kyushu University. He served as an Air Liquide industrial chair on hydrogen structural materials and fracture during 2010 – 2014 concurrent with professor at Kyushu University. He moved to International Institute for Carbon-Neutral Energy Research (WPI-I2CNER), Kyushu University in 2014. Then, he has studied hydrogen embrittlement with Professor Petros Sofronis who is a professor at University of Illinois at Urban Champaign. He published more than 90 refereed papers. His two papers regarding fretting fatigue won outstanding paper awards in 2007 and 2008, respectively. He has given 6 invited talks and 4 keynote speeches at international conferences.

Prof. Kubota served as editorial advisory boards for some mechanical engineering journals. He has served as a board member to Society for Materials Science, Japan since 2016.

Xuesong Cui is a Master course student in Graduate School of Mechanical Engineering, Kyushu University. He studies strength of materials as well as hydrogen embrittlement.

Hiroshi Wakabayashi is a Section Manager at Research and Development Section. Engineering Development Department, NAGANO KEIKI CO., LTD. who is a pressure gauges and pressure sensors company. He is responsible for product development as well as technology development for pressure sensors.

Yasuhisa Tanaka is a young engineer at Sensor Application Engineering Department, Mechanisms Design Section, NAGANO KEIKI CO., LTD. He is in charge of design of pressure sensors for general industry. He also designs high-pressure hydrogen pressure sensors.

Ryoauke Komoda was born in Fukuoka, Japan, in 1989. He received BS, MS and PhD in Engineering from Kyushu University in Fukuoka, Japan in 2012, 2014 and 2017, respectively. His specialties are fatigue and fracture, fretting fatigue and hydrogen embrittlement. He works as a Post-doctoral Research Associate at International Institute for Carbon-Neutral Energy Research (WPI-I2CNER), Kyushu University in Fukuoka, Japan from 2017. Currently, he studies the effect of gas impurities contained in hydrogen gas on hydrogen embrittlement. Dr. Komoda belongs to The Japan Society of Mechanical Engineering (JSME), The Society of Material Science, Japan (JSMS) and The Iron and Steel Institute of Japan (ISIJ).